Matrix-Isolation Infrared and Theoretical Study of the Reaction of VCl_4 with CH_3OH

Dana Sabestinas[†] and Bruce S. Ault*

Department of Chemistry, University of Cincinnati, P.O. Box 210172, Cincinnati, Ohio 45221

Received: December 5, 2003; In Final Form: February 18, 2004

The matrix isolation technique, combined with infrared spectroscopy and theoretical calculations, has been used to investigate VCl_4, as well as its reactions with CH_3OH and its isotopomers. The infrared spectrum of VCl_4 in solid argon showed an intense doublet at 474 and 501 cm^{-1}, which is indicative of a splitting of the triply degenerate stretching mode in T_d symmetry due to Jahn−Teller distortion. Density functional theory (DFT) calculations (UB3LYP/6-311++g(d,2p)) reproduced this splitting very well. The calculated structure had four equal V−Cl bonds, but with two Cl−V−Cl angles equal to 110.8° and two angles equal to 106.9°. Using twin-jet deposition, the initial intermediate in the reaction of VCl_4 with CH_3OH was identified as a 1:1 molecular complex, characterized by perturbations to the V−Cl, C−O, and O−H stretching modes. This complex was destroyed by near-UV irradiation, producing the novel Cl_3VOCH_3 species and cage-paired HCl. Merged-jet co-deposition of CH_3OH and VCl_4, with a room-temperature reaction zone, led to almost-complete conversion to Cl_3VOCH_3. This species was identified by use of isotopic labeling, the observation of HCl as an additional reaction product, and by comparison to DFT calculations. In addition, a large yield of CH_3Cl was observed.

Introduction

High-valency transition-metal oxo compounds, including $OVCl_3$ and $CrCl_2O_2$, are very strong oxidizing agents and are known to oxidize a wide range of organic substrates.[1,2] This oxidizing power has applications in catalysis and organic synthesis. Despite the utility of these reagents, the mechanism of oxidation is not well understood, although progress has been made in recent years. The reaction chemistry of VCl_4 might be expected to be similar to that of its oxo counterpart, $OVCl_3$; yet, two significant differences are present. First is the presence of the oxo group, and the second is the presence of an unpaired electron on the vanadium center in VCl_4. How these two factors affect the chemistry of VCl_4 is not well understood.

The matrix isolation technique[3−5] was developed to facilitate the isolation and spectroscopic characterization of reactive intermediates. This approach has been applied to the study of a wide range of species, including radicals, weakly bound molecular complexes, and molecular ions. A recent series of matrix isolation studies[6−10] has examined the reactions of both $OVCl_3$ and $CrCl_2O_2$ with small molecules, including H_2O, CH_3OH, CH_3SH, and NH_3. For each system, a sequence of intermediate species was observed, from the initially formed 1:1 molecular complex to the thermally or photochemically induced HCl elimination product. In addition, a recent matrix isolation electron spin resonance (ESR) study of VCl_4 in several different matrices was performed, in search of indications of Jahn−Teller distortion as a consequence of the lone unpaired electron.[11] No infrared studies have been conducted on VCl_4 in cryogenic matrices, and no recent theoretical studies have been conducted. Consequently, a matrix-isolation infrared spectroscopic study was undertaken, both to characterize the infrared spectrum of VCl_4 in solid argon and to explore the range of reaction products of VCl_4 with CH_3OH in argon matrices. Theoretical calculations were performed in support of the experimental work.

Experimental Details

All the experiments in this study were conducted on a conventional matrix isolation apparatus that has been described previously.[12] Vanadium(IV) chloride (VCl_4, from Aldrich) was introduced into the vacuum system by placing a few drops of the neat liquid in a small stainless-steel sidearm that was connected to the deposition line through a needle valve to an Ultratorr tee. The needle valve was opened slightly (to allow a fraction of the vapor pressure of VCl_4 at room temperature to be entrained in flowing argon), carried to the cold window, and deposited. CH_3OH (Aldrich), as well as CD_3OH and $^{13}CH_3OH$ (both from Cambridge Isotope Laboratories, 99% isotopic enrichment), were also introduced as the vapor above the room-temperature liquid, after repeated freeze−pump−thaw cycles. Argon was used as the matrix gas in all experiments, and it was used without further purification.

Matrix samples were deposited in both the twin-jet and merged-jet modes. In the former, the two gas samples were deposited from separate nozzles onto the 14 K cold window, allowing for only a very brief mixing time prior to matrix deposition. Several of these matrices were subsequently warmed to 33−35 K, to permit limited diffusion, and then recooled to 14 K and additional spectra recorded. In addition, most of these matrices were irradiated with the H_2O/Pyrex-filtered output of a 200 W medium-pressure mercury arc lamp, after which time additional spectra were recorded. Irradiation times of 1−3 h were used.

Many experiments were conducted in the merged-jet mode,[13] in which the two deposition lines were joined with an Ultratorr tee at a distance from the cryogenic surface, and the flowing gas samples were permitted to mix and react during passage through the merged region. The length of this region was

* Author to whom correspondence should be addressed. E-mail: bruce.ault@uc.edu, Ault@email.uc.edu.
† NSF-REU student from Kings College, Wilkes Barre, PA.

10.1021/jp037726c CCC: $27.50
Published on Web 03/19/2004

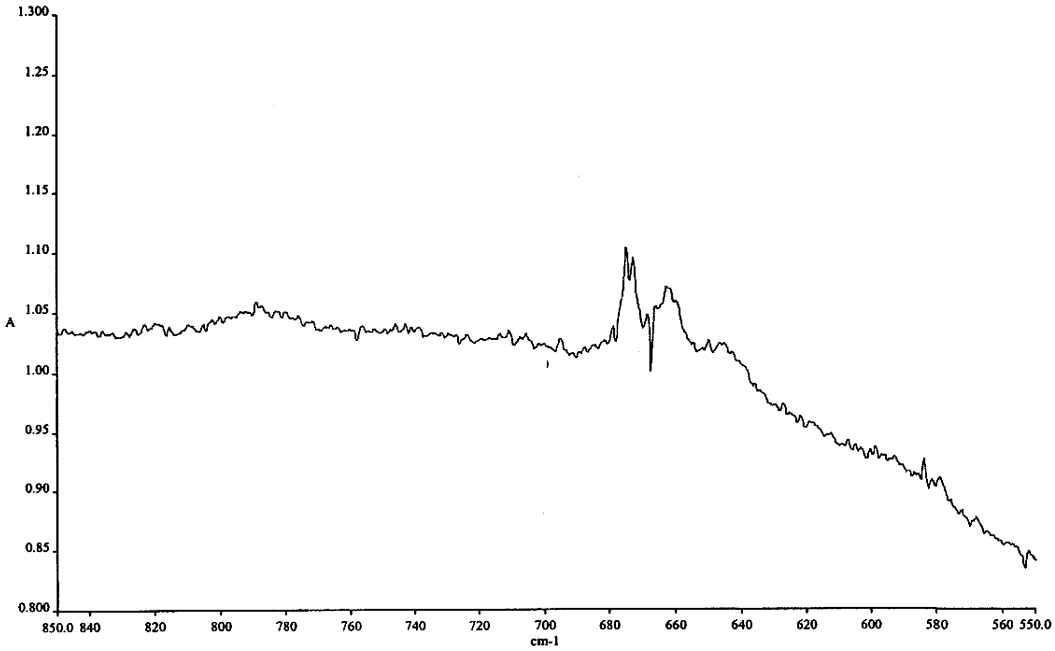

Figure 1. Difference spectrum, before and after irradiation, of a matrix prepared by the twin-jet co-deposition of a sample of Ar/VCl_4 with a sample of Ar/CH_3OH. The feature at 674 cm^{-1} is due to the photoinduced reaction of CH_3OH with impurity $OVCl_3$, whereas the feature at 667 cm^{-1} is due to the photoinduced reaction of CH_3OH with VCl_4.

variable (10−90 cm). In both twin-jet and merged-jet modes, matrices were deposited at the rate of 2 mmol/h from each sample manifold onto the cold window. Final spectra were recorded on a Perkin−Elmer Spectrum One Fourier transform infrared spectrometer at a resolution of 1 cm^{-1}.

Theoretical calculations were performed on several possible intermediates in this study, using the Gaussian 98W suite of programs.[14] Several different model chemistries were used, including Hartree−Fock and density functional calculations. These calculations were used to locate energy minima, determine structures, and calculate vibrational spectra. Final calculations with full geometry optimization used unrestricted B3LYP with the 6-311++g(d,2p) basis set, after initial calculations with smaller basis sets were run to approximately locate energy minima.

Experimental Results

Prior to any co-deposition experiments, blank experiments were run on each of the reagents used in this study. In each case, the blanks were in good agreement with literature spectra,[15,16] where available, and with blanks run previously in this laboratory. With VCl_4 samples, reproducibility was challenging, because of difficulties in precisely controlling the flow through the needle valve. In addition, a low level of $OVCl_3$ impurity[17] was present in all VCl_4 experiments, as were weak bands that were due to HCl impurity.[18]

VCl_4 Experiments. Multiple experiments were conducted in which VCl_4 was deposited into solid argon over a wide range of concentrations. The quantitative concentrations could not be determined; however, the relative concentration from one experiment to the next could be determined by measuring the rate of growth of the VCl_4 absorptions. In all experiments, a very strong pair of bands was observed at 474 and 501 cm^{-1}. These bands were themselves split slightly, because of different isotopic combinations of ^{35}Cl and ^{37}Cl. The relative intensities of these two bands remained constant over a wide range of experiments and sample concentrations, and also when the matrices were annealed. In addition, much weaker but discernible bands at 509 and 1038 cm^{-1} that were due to impurity $OVCl_3$ were observed throughout.

VCl_4 + CH_3OH. In an initial twin-jet experiment, a sample of Ar/VCl_4 was co-deposited with a sample of Ar/CH_3OH (Ar/CH_3OH ratio of 500). After deposition, weak features were observed in the spectrum, at 418, 447, 996, 1001, 3599, and 3607 cm^{-1} (hereafter referenced as set A). The latter two pairs appeared as slightly split doublets. When this matrix was gently annealed to ∼30 K, and then recooled to 14 K, all these bands grew slightly (10%−15%) and at the same rate. This matrix was then irradiated by the output of a medium-pressure mercury arc lamp, using a Pyrex/H_2O filter that transmitted wavelengths of $\lambda > 300$ nm. After 1 h of irradiation, all of the aforementioned set A bands were completely absent, and new bands were observed at 423, 667, 1062, 1144, 1423, 1443, 2758, and 2773 cm^{-1}. All of these bands were weak as well, but nonetheless clearly distinct from the spectral noise. All of these bands, except for the doublet at 2758, 2773 cm^{-1}, will be referenced as set B. A portion of this spectrum is shown in Figure 1.

This experiment was repeated on several occasions, using different sample concentrations of both reagents. Concentrations as diluted as $Ar/CH_3OH = 1000$ were used. In each case, the set A bands were observed upon initial deposition, with intensities consistent with sample concentration (i.e., when the concentration of CH_3OH was reduced by a factor of 2, the set A bands were reduced by a similar factor). Each matrix was irradiated with light of $\lambda > 300$ nm, and the set A bands were destroyed by irradiation in each experiment. The set B bands grew in, along with the 2758, 2773 cm^{-1} doublet. The bands of set B maintained a constant intensity ratio, with respect to each other, from one experiment to the next, whereas their absolute intensities also varied directly with the intensities of the initial set A bands (i.e., when set A was relatively more intense before irradiation, the set B bands were relatively more intense after irradiation).

The reaction of VCl_4 and CH_3OH was also explored in a series of merged-jet experiments. In the initial experiments, a short, 10-cm room-temperature merged region was used. When

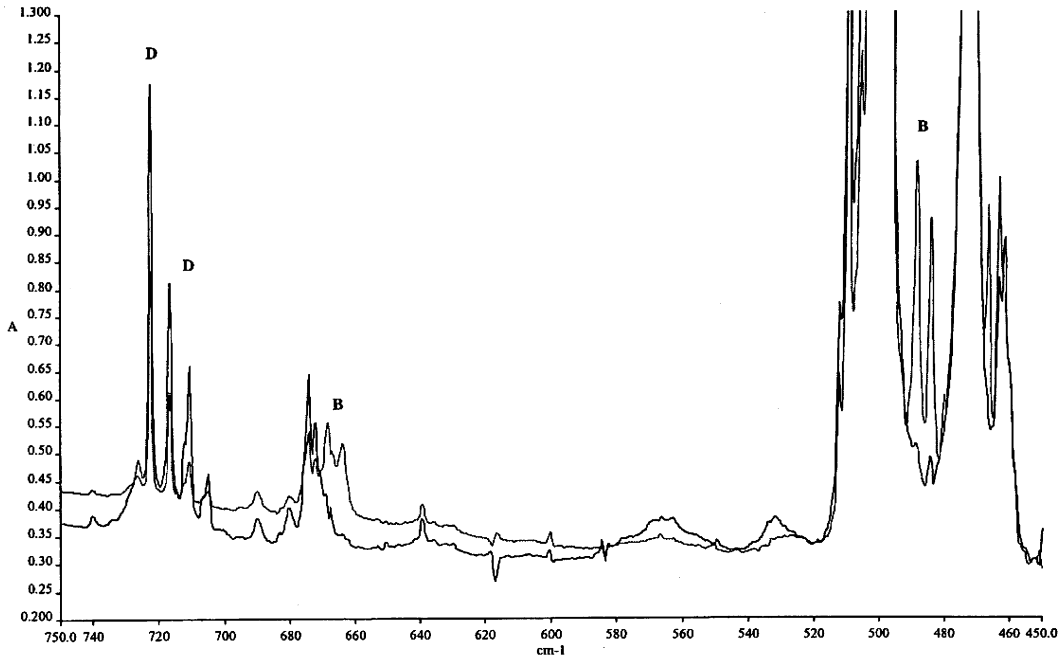

Figure 2. Infrared spectra of two matrices prepared by the twin-jet co-deposition of a sample of Ar/VCl_4 with a sample of Ar/CH_3OH, at two different relative concentrations. Bands labeled B are due to Cl_3VOCH_3 and bands labeled D are due to CH_3Cl and $HCl{\cdot}CH_3Cl$.

a sample of Ar/VCl_4 was co-deposited in this manner with an Ar/CH_3OH sample ($Ar/CH_3OH = 500$), very different spectral features were observed, compared to the analogous twin-jet experiment. First, bands due to parent CH_3OH were completely absent, whereas bands to parent VCl_4 were diminished in intensity. Many new bands were observed throughout the spectrum, some with quite high intensity. Most intense was a feature at 2888 cm^{-1}, along with moderately intense features between 2800 and 2855 cm^{-1} (hereafter referenced as set C). In addition, bands were observed at 425, 668, 1062, 1423, and 1443 cm^{-1}, which are very close to the set B bands in the twin jet experiments. Moreover, they showed the same relative intensities as the set B bands and are likely due to the same product species. In addition, bands at 484, 488, and 2944 cm^{-1} consistently maintained a constant intensity ratio, relative to these merged-jet bands, and very probably are also members of set B. The overall yield of these set B bands was higher in the merged-jet experiment, and because the 2944 cm^{-1} band was weak, it would not have been observed in the twin-jet experiments. The 484 and 488 cm^{-1} bands were hidden by intense bands due to parent VCl_4 in the twin-jet experiments, but were detectable with the reduced intensity of the parent VCl_4 bands in the merged-jet experiments. Additional moderately intense product bands in the merged-jet experiment were observed near 720 (sharp multiplet), 1014, 1350, 2746 (multiplet), 2964, 3032, and 3040 cm^{-1} (hereafter referenced as set D). Finally, weaker product bands were observed near 2528 and 2664 cm^{-1}. (See Figure 2.)

This experiment was repeated several times using the short room-temperature merged-jet line and different sample concentrations. When a lower VCl_4 level was used with a higher CH_3OH level, parent bands of VCl_4 were absent, whereas parent bands of CH_3OH were apparent. All of the product bands described in the preceding paragraph were observed, although the different groupings had different relative intensities, with respect to other groupings. The set C bands were still very intense. However, the relative yields of the set B and set D bands changed as a function of sample concentration. When a high level of CH_3OH was used with a lower level of VCl_4, the set D bands were relatively more intense than the set B bands. Conversely, when a high level of VCl_4 was used with a lower level of CH_3OH, the set D bands were relatively less intense than the set B bands. At very high VCl_4 levels, the set D bands were barely visible.

Additional experiments were run using a somewhat longer merged-jet region (~50 cm), to increase mixing and reaction time. Several experiments were run, at several different sample concentrations. The qualitative results were quite similar to those obtained at the same sample concentrations with the short merged region. The yields of the set B and set D bands were increased slightly, but no additional product bands were observed. Inasmuch as apparently complete reaction was occurring with the merged region held at room temperature, no experiments were performed in which the merged region was heated above room temperature.

Isotopic Studies. Several experiments were conducted in which samples of Ar/VCl_4 were co-deposited with samples of $Ar/^{13}CH_3OH$. All of these experiments were conducted in the merged-jet mode, which was shown (previously) to produce a much higher yield of reaction product. In these experiments, the set C bands were observed between 2800 and 2888 cm^{-1}, unshifted relative to the normal isotopic experiments. Infrared absorptions were noted near each of the set B and set D bands, with very similar relative intensities. These, however, were generally shifted several wavenumbers, relative to the normal isotope. For example, the set B band observed at 668 cm^{-1} for the normal isotope shifted to 663 cm^{-1}, whereas the 2944 cm^{-1} band shifted to 2934 cm^{-1}. The band positions for the set B bands are listed in Table 1.

Experiments were also conducted in which samples of Ar/VCl_4 were co-deposited with samples of Ar/CD_3OH. All of these experiments were conducted in the merged-jet mode. In these experiments, the set C bands were seen between 2800 and 2888 cm^{-1}, again unshifted relative to the normal isotopic experiments. In addition, numerous new product bands were observed, most of which were shifted (as expected) from the normal isotopic experiments (see Figure 3). Multiple experiments were conducted over a range of sample concentrations. Based on the intensity behavior of each band as a function of sample concentration, all of the product bands could be sorted into two

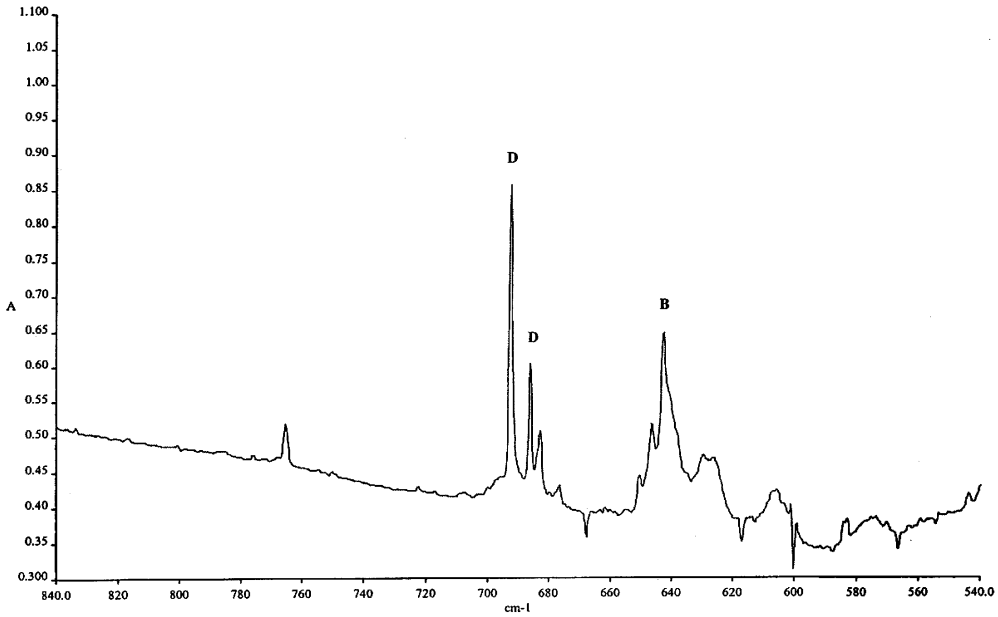

Figure 3. Infrared spectrum of a matrix prepared by the merged-jet co-deposition of a sample of Ar/VCl_4 with a sample of Ar/CD_3OH. Bands labeled B are due to Cl_3VOCH_3, and bands labeled D are due to CH_3Cl and $HCl{\cdot}CH_3Cl$.

TABLE 1: Band Positions and Assignments for Argon Matrix Isolation of Cl_3VOCH_3

Band Position (cm^{-1})			
Cl_3VOCH_3	$Cl_3VO^{13}CH_3$	Cl_3VOCD_3	assignment
425	425	425	VCl_3 symmetric stretch
486	486	486	VCl_3 antisymmetric stretch
668	663	642	V−O stretch
1423	1420		CH_3 symmetric bend
1444	1444	1053	CH_3 antisymmetric bend
2944	2934	2167	CH_3 antisymmetric stretch

sets, analogous to sets B and D, as discussed previously. The set B bands are also listed in Table 1.

Results of Calculations

Density functional theory (DFT) calculations focused on energy minima, structures, and vibrational frequencies for parent VCl_4, as well as for possible reaction products. For VCl_4, the minimum energy structure was a distorted tetrahedron, which consisted of four V−Cl bands of equal length (2.145 Å), with two Cl−V−Cl angles of 106.9° and two of 110.8°. With this distorted structure, three intense V−Cl stretching modes were calculated, although two were essentially degenerate.

Previous studies[6−10] have identified a molecular complex as the initial product in similar twin-jet reactions where the reaction time is very short. Consequently, possible structures for a 1:1 complex were explored computationally. One structure, shown in Figure 4, was optimized to a stable minimum at all levels of theory. This structure has a relatively short V−O distance (2.19 Å), which was indicative of coordination of the oxygen to the vanadium(IV) center. At the same time, the distance between the hydroxyl hydrogen and the nearest chlorine was calculated to be 2.54 Å, which suggested weak hydrogen bonding as well. As discussed below, this is consistent with the spectral changes observed upon complex formation. The energy required for complex formation (ΔE°_{298}) was calculated to be −6.00 kcal/mol at the UB3LYP/6-311++g(d,2p) level of theory.

Of interest also was Cl_3VOCH_3, by analogy to the known reaction of $OVCl_3$ with CH_3OH. Cl_3VOCH_3 was optimized to a stable energy minimum at all levels of theory used, including unrestricted B3LYP/6-311++g(d,2p), which was the highest

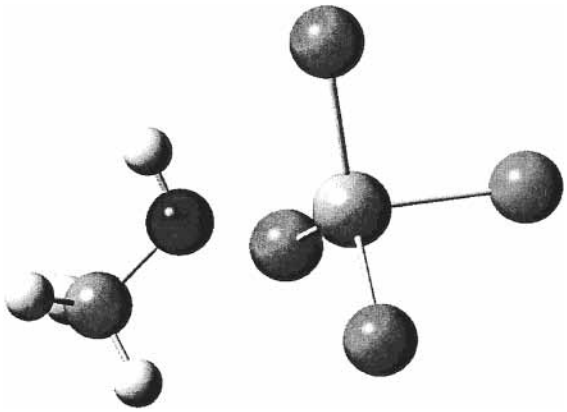

Figure 4. Representation of the optimized structure computed for the 1:1 complex $Cl_4V{:}CH_3OH$, computed at the UB3LYP/6-311++g-(d,2p) level of theory (see also Table 4).

TABLE 2: Calculated Key Structural Parameters for Cl_3VOCH_3 and $Cl_2V(O)OCH_3$[a]

	Value	
parameter	Cl_3VOCH_3	$Cl_2V(O)OCH_3$
R_{V-Cl}[b]	2.171 Å	2.169 Å
$R_{V=O}$		1.554 Å
R_{V-O}	1.721 Å	1.719 Å
R_{C-O}	1.428 Å	1.420 Å
R_{C-H}[b]	1.090 Å	1.092 Å
α(Cl−V−Cl)[b]	110°	109°
α(Cl−V−O)[b]	106°	109°
α(V−O−C)	138.4°	135.7°
α(H−C−H)[b]	110°	110°

[a] Calculated at the UB3LYP/6-311++g(d,2p) level of theory; from ref 8. [b] Average of three values.

level used. The resulting structure was reasonable; the key geometric parameters are listed in Table 2 and the structure is shown in Figure 5. The V−O−C bond angle of 138.4° is a notable feature. This angle is much greater than would be anticipated for a single-bond linkage (i.e., sp^3 hybridization at the O atom) and suggests partial multiple bond character in the V−O bond. Vibrational frequencies were also calculated, for the normal isotopic species as well as for the ^{13}C and $-CD_3$

TABLE 3: Experimental and Theoretical[a] Vibrational Frequencies (UB3LYP/6-311++g(d,2p)) for Cl_3VOCH_3 and Its Isotopomers

Cl_3VOCH_3			$Cl_3VO^{13}CH_3$		Cl_3VOCD_3		
calculated (cm^{-1})	*I* (calculated)	experimental (cm^{-1})	calculated shift (cm^{-1})	experimental shift (cm^{-1})	calculated shift (cm^{-1})	experimental shift (cm^{-1})	assignment
462	117	425	0	0	0	0	VCl_3 symmetric stretch
479	149	486	0	0	0	0	VCl_3 antisymmetric stretch
660	102	668	−8	−5	−29	−26	V−O stretch
1068	303	1062	−15	−11	4		C−O stretch
1144	2		−8		−264		CH_3 rock
1166	43		−8		−273		CH_3 rock
1464	7	1423	−4	−3	−360		CH_3 symmetric bend
1486	13	1444	−2		−414	−391	CH_3 antisymmetric bend
1486	5		−2	0	−409		CH_3 antisymmetric bend
3025	26		−2		−858		CH_3 symmetric stretch
3101	9		−12		−800		CH_3 antisymmetric stretch
3115	10	2944	−12	−10	−803	−777	CH_3 antisymmetric stretch

[a] Theoretical frequencies are unscaled.

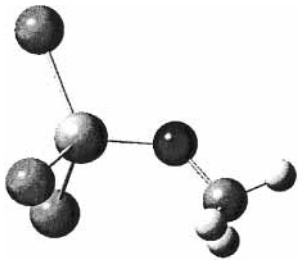

Figure 5. Representation of the optimized structure computed for Cl_3VOCH_3, computed at the UB3LYP/6-311++g(d,2p) level of theory (see also Table 2).

TABLE 4: Calculated and Experimental Band Positions and Assignments for the 1:1 Complex of VCl_4 with CH_3OH[a]

complex	V−Cl stretch (cm^{-1})	C−O stretch (cm^{-1})	O−H stretch (cm^{-1})
$VCl_4 \cdot CH_3OH$	418, 447	996, 1001	3599, 3607
parent band	474, 501	1031	3667
experimental shift	−56, −54	−32[b]	−64[b]
calculated shift[c]	−57, −52	−29	−47

[a] Only for normal isotopic species; only the merged jet experiments were run with $^{13}CH_3OH$ and CD_3OH (see text). [b] Using mean of site split doublets. [c] Calculated at the UB3LYP/6-311++g(d,2p) level of theory.

isotopomers. These frequencies and isotopic shifts are listed in Table 3. In addition, values of thermodynamic quantities (*E*, *H*, and *G*) were calculated at this level of theory, which allowed estimates to be made of the ΔE, ΔH, and ΔG values for reactions of interest. Of note, ΔG°_{298} for the reaction of VCl_4 with CH_3OH was calculated to be approximately −4.3 kcal/mol, whereas the ΔG°_{298} value for the decomposition of Cl_3VOCH_3 to CH_3Cl and Cl_2VO was +19.3 kcal/mol. Although these calculations are not at the highest levels, they provide some guidance as to the feasibility of reactions of interest in this system. Calculations were also performed for potential secondary products, including Cl_2VO, that might be formed in this reaction.

Discussion

The infrared spectrum of VCl_4 in argon matrices has not been reported to date, although Weltner et al. reported the ESR spectrum in 2000.[11] They detected evidence of Jahn−Teller distortion away from a tetrahedral structure that was due to the unpaired electron on the vanadium center. The distortion was most apparent in solid H_2 and neon, whereas both distorted and isotropic spectra were observed in argon. The infrared spectra obtained here in argon show two very intense bands: at 474 and 501 cm^{-1}. Each showed splittings that were due to chloride isotopes in natural abundance. A tetrahedral structure would have only a single, triply degenerate, infrared active V−Cl stretching mode in this region, which is inconsistent with the observed spectrum. The persistence of two intense bands over a range of VCl_4 concentrations, as well as the fact that almost-identical spectra were obtained upon sample annealing, suggests that the splitting is a fundamental property of VCl_4 in solid argon and not a consequence of aggregation and/or site splitting. Jahn−Teller distortion is expected to distort the molecule axially, splitting the triply degenerate mode into three V−Cl stretching modes. This is apparently inconsistent with the observed spectrum. However, unrestricted DFT calculations show that two of the three modes are almost degenerate (the lower-energy pair of bands), with a separation of 0.06 cm^{-1}. With the closely spaced, overlapping multiplet that is due to Cl isotopes, such a splitting would not be detectable. The separation between the upper band (509 cm^{-1}) and the lower bands (473 cm^{-1}) was calculated to be 36 cm^{-1}, which is in good agreement with the observed separation of 27 cm^{-1}. Thus, the observed spectrum is well-explained by an axially distorted structure, as proposed by Weltner et al.[11]

Identification of Products

Twin-jet deposition of VCl_4 and CH_3OH into argon matrices led to the observation of four weak bands (two of which were doublets)—the set A bands—as listed in Table 4. These bands were formed under the conditions of the shortest reaction time and the lowest reaction temperature, namely in twin-jet deposition experiments where mixing of the two reactants occurs on the surface of the condensing matrix. This indicates that species A is the initial intermediate in the reaction between VCl_4 and CH_3OH. Furthermore, although the yield of species A was quite low during deposition, bands due to species A grew when the matrix was annealed to 33 K. Thus, the barrier to formation of species A from the isolated reactants must be very low. This is indicative of the formation of a molecular complex between the two subunits,[19] and the low sample concentrations in solid argon suggest that the stoichiometry of the complex is 1:1. This is consistent with theoretical calculations (see previous discussion) that predict the stability of such a complex.

Spectroscopically, complex formation would be manifested by a shifting of certain vibrational modes of the two subunits, particularly modes that involve atoms at the site of complexation. Because CH_3OH is known to serve as a proton donor in

hydrogen-bonding interactions and VCl_4 has four very electronegative ligands, hydrogen-bond formation is reasonable. Coordination through the O atom of CH_3OH to the highly positive vanadium center on VCl_4 is also possible. The calculated structure (Figure 4) shows that both types of interactions help to stabilize the complex. Spectroscopically, the two vibrational modes of the CH_3OH subunit most perturbed by the formation of the complex were the O−H stretch (shifted from 3667 cm^{-1} in the parent to 3603 cm^{-1} in the complex) and the C−O stretch (shifted from 1031 cm^{-1} in the parent to 999 cm^{-1} in the complex), as shown in Table 4. These observations are consistent with oxygen coordination and at least a weak hydrogen-bonding interaction.[20] In addition, two perturbed, shifted V−Cl stretching modes were observed. Strong support for these assignments comes from the calculations, as shown in Table 4. The C−O stretch in the complex was calculated to occur at 1012 cm^{-1}, very near the experimental band position. The shift relative to the parent was calculated to be −29 cm^{-1}, whereas the experimental shift was −32 cm^{-1}. Similarly good agreement was observed for the O−H and V−Cl stretching band shifts. All of these observations point to the identification of species A as a molecular complex between CH_3OH and VCl_4, the initial intermediate for this pair of reactants.

The initial complex was destroyed by mercury arc irradiation while trapped in the cryogenic matrix, resulting in the bands in set B plus the doublet at 2758, 2773 cm^{-1}. Set B was also formed in the room-temperature merged-jet reaction of VCl_4 with CH_3OH, in much higher yield, and accompanied by the production of bands in set C. The bands in set C can be readily assigned to matrix-isolated HCl monomers and dimers by comparison to authentic matrices that contain HCl, as well as to the literature.[18] This is consistent with a lack of ^{13}C and $-CD_3$ shift for these bands, assuming that the HCl forms from the hydroxyl H atom on CH_3OH. The bands 2758 and 2773 cm^{-1} formed after irradiation in the twin-jet experiments showed similar isotopic behavior to HCl, with a lack of ^{13}C and $-CD_3$ shift. However, the bands at 2758, 2773 cm^{-1} were ∼100 cm^{-1} lower in energy than those of matrix-isolated HCl, which suggests that they are due to hydrogen-bonded HCl. This doublet was produced at the same time as set B, and they both result from the photodestruction of the initial hydrogen-bonded complex (species A). Thus, species B and the species responsible for the 2758, 2773 cm^{-1} doublet are very likely trapped within the same matrix cage. If HCl is formed in the photoreaction and is cage-paired with species B, then it would be expected to interact weakly (e.g., form a hydrogen bond) with species B. In the thermal, merged-jet reaction, the HCl that is produced can separate from species B in the gas phase prior to matrix deposition and is trapped primarily as free HCl. Thus, species C is identified as free, matrix-isolated HCl, whereas the doublet at 2758, 2773 cm^{-1} is identified as HCl that is weakly hydrogen-bonded to species B.

Species B was produced in relatively low yield by irradiation of the matrix after twin-jet deposition and in substantially higher yield by merged-jet deposition. Formation after irradiation of the 1:1 complex, with concomitant HCl formation, strongly suggests the formation of Cl_3VOCH_3, which is a species that is a methoxy derivative of the parent VCl_4. Chemical intuition suggests that such a species should be stable. Also, as noted previously, DFT calculations predict that Cl_3VOCH_3 should be stable, and the calculated spectrum agrees very well with the observed bands of set B, including isotopic shifts (see the "Band Assignments" section later in this work). In the analogous reactions of $CrCl_2O_2$, $OVCl_3$, and $TiCl_4$ with CH_3OH, similar HCl elimination reactions were observed, leading in each case to a methoxy derivative of the parent compound. Thus, species B is identified as the HCl elimination product of the initial complex, Cl_3VOCH_3. Note that the band positions for several of the vibrational modes of species B were shifted slightly (1−2 cm^{-1}) in the twin-jet experiments, relative to the merged-jet experiments. This is due to the fact that $Cl_2V(O)OCH_3$ is produced and cage-paired with HCl and $Cl_2V(O)OCH_3$ in the twin-jet experiments, whereas $Cl_2V(O)OCH_3$ is trapped as the uncomplexed molecule in the merged-jet experiments. Weak interactions between the cage-paired species leads to small perturbations and band shifts (as described previously for cage-paired HCl). Band positions and assignments for Cl_3VOCH_3 are collected in Table 1 (using the merged-jet band positions), whereas comparison to DFT calculated spectra and isotopic shifts is made in Table 3.

The bands due to species D were *not* formed in the twin-jet experiments after irradiation, but were quite clear and distinctive in the merged-jet experiments. These bands are readily assigned by comparison to authentic spectra, to CH_3Cl[21] and the HCl complex[22] of CH_3Cl. Not only did band positions match literature values, but identical isotopic shifts also were observed (for the mechanism of formation of CH_3Cl, see below). Finally, the two product bands detected at 2528 and 2664 cm^{-1} are due to the known 1:1 complexes[22,23] of HCl with CH_3OH and H_2O (which are present as a low-level impurity in all experiments).

Band Assignments for Cl_3VOCH_3

The band assignments for Cl_3VOCH_3 are straightforward, based on comparison to the previously studied $Cl_2V(O)CH_3$ and to the theoretical calculations. In fact, it is remarkable how close the product bands for Cl_3VOCH_3 and $Cl_2V(O)OCH_3$ are to each other. For example, the V−O stretch in $Cl_2V(O)OCH_3$ was reported at 674 cm^{-1}, whereas the analogous mode for Cl_3VOCH_3 was observed here at 668 cm^{-1}. Vibrations of the $-CH_3$ unit for both species were quite similar, as might be expected. Table 3 lists the calculated band positions for Cl_3VOCH_3 at the UB3LYP/6-311++g(d,2p) level of theory, the experimental band positions, as well as the calculated and experimental ^{13}C and $-CD_3$ isotopic shifts. As can be seen, the overall agreement is quite good. Of course, not all of the bands due to Cl_3VOCH_3 were observed. Several were calculated to be quite weak, while others were in calculated in regions overlapped by parent bands. Nonetheless, 7 out of 13 fundamentals predicted above 400 cm^{-1} were observed; all were within a few percent of the calculated fundamentals (calculated frequencies are unscaled). More importantly, the isotopic shifts were reproduced very well, lending support to these assignments.

Further Considerations

CH_3Cl and the HCl complex of CH_3Cl were observed previously[8,24] as thermal decomposition products in the merged-jet pyrolysis (at temperatures of $T > 100$ °C) of Cl_3TiOCH_3 and $Cl_2V(O)OCH_3$. In the present experiments, CH_3Cl is formed when the merged or reaction region was held at room temperature. Moreover, the relative yields of the products Cl_3VOCH_3 (set B) and CH_3Cl (set D) varied strongly in these experiments, as a function of the precursor sample concentration. As described previously, CH_3Cl was strongly favored at low VCl_4/CH_3OH ratios, whereas Cl_3VOCH_3 was strongly favored at high VCl_4/CH_3OH ratios. Thus, concentration ratio rather than temperature seemed to be the determining factor in the formation of CH_3Cl. The most likely possibility is the reaction of a first molecule of CH_3OH with VCl_4 to form Cl_3VOCH_3 and HCl, followed

by the reaction of a second molecule of CH_3OH with the product Cl_3VOCH_3 to form $Cl_2V(OCH_3)_2$, which then rapidly decomposes to $2CH_3Cl + VO_2$. This latter product is not volatile and would not survive passage through the deposition line to the cold window and, hence, would not be detected. This conclusion is supported by theoretical calculation of the thermochemistry of the direct decomposition reaction $Cl_3VOCH_3 \rightarrow CH_3Cl + Cl_2VO$. This reaction was calculated to have a Gibbs free energy of $\Delta G^\circ_{298} = +19.3$ kcal/mol at the UB3LYP/6-311++g(d,2p) level. This value suggests that direct decomposition at room temperature is unlikely and that a biomolecular chemical reaction is the more-probable source of CH_3Cl. In comparison, the reaction $VCl_4 + CH_3OH \rightarrow Cl_3VOCH_3 + HCl$ was calculated to have $\Delta G^\circ_{298} = -4.3$ kcal/mol at this level of theory (and this reaction was, in fact, observed).

A comparison of the reaction chemistry of VCl_4 and $OVCl_3$ was another goal of this study. Indeed, the primary reaction processes were very similar. In both cases, twin-jet deposition led to a small yield of the 1:1 complex, which eliminated HCl upon irradiation with light of $\lambda > 300$ nm. Both VCl_4 and $OVCl_3$ reacted extensively with CH_3OH when room-temperature merged-jet deposition was used, which led to Cl_3VOCH_3 and $Cl_2V(O)OCH_3$, respectively. As noted previously, the spectra of these two species were very similar. Also, the calculated geometric parameters for the two species, including the V−O−C angle, are very similar, as shown in Table 2. These observations suggests that the role of the oxo group of $OVCl_3$ in this case is not great, and the lone unpaired electron on VCl_4 is not dominating the reaction chemistry, at least in the reaction with CH_3OH. Further exploration of the reaction chemistry of VCl_4, and comparison with $OVCl_3$, currently is underway.

Acknowledgment. The National Science Foundation is gratefully acknowledged for their support of this research (through Grant No. CHE02-43731). D.S. also gratefully acknowledges support from NSF-REU program at the University of Cincinnati (through Grant No. CHE-0097726). David Kayser is gratefully acknowledged for his assistance with several experiments.

References and Notes

(1) Crans, D. C.; Chen, H.; Felty, R. A. *J. Am. Chem. Soc*. **1992**, *114*, 4543.
(2) Yajima, A.; Matsuzaki, R.; Saeki, Y. *Bull Chem. Soc. Jpn*. **1978**, *51*, 1098.
(3) Craddock, S.; Hinchliffe, A. *Matrix Isolation*; Cambridge University Press: Cambridge, U.K., 1975.
(4) Hallam, H. E., *Vibrational Spectroscopy of Trapped Species*; Wiley: New York, 1973.
(5) Andrews, L., Moskovitz, M., Eds. *Chemistry and Physics of Matrix Isolated Species*; Elsevier Science Publishers: Amsterdam, 1989.
(6) Ault, B. S. *J. Am. Chem. Soc*. **1998**, *120*, 6105.
(7) Anderson, S. R.; Ault, B. S. *J. Phys. Chem. A* **2002**, *106*, 1419.
(8) Ault, B. S. *J. Phys. Chem. A* **1999**, *103*, 11474.
(9) Ault, B. S. *J. Phys. Chem. A* **2001**, *105*, 4758.
(10) Subel, B. L.; Kayser, D. A.; Ault, B. S. *J. Phys. Chem. A* **2002**, *106*, 4998.
(11) Graham, J. T.; Li, L.; Weltner, W., Jr. *J. Phys. Chem. A* **2000,** *104*, 9302.
(12) Ault, B. S. *J. Am. Chem. Soc*. **1978**, *100*, 2426.
(13) Carpenter, J. D.; Ault, B. S. *J. Phys. Chem.* **1991**, *95*, 3502.
(14) Frisch, M. J.; Trucks, G. W.; Schlegel, H. B.; Scuseria, G. E.; Robb, M. A.; Cheeseman, J. R.; Zakrzewski, V. G.; Montgomery, J. A., Jr.; Stratmann, R. E.; Burant, J. C.; Dapprich, S.; Millam, J. M.; Daniels, A. D.; Kudin, K. N.; Strain, M. C.; Farkas, O.; Tomasi, J.; Barone, V.; Cossi, M.; Cammi, R.; Mennucci, B.; Pomelli, C.; Adamo, C.; Clifford, S.; Ochterski, J.; Petersson, G. A.; Ayala, P. Y.; Cui, Q.; Morokuma, K.; Malick, D. K.; Rabuck, A. D.; Raghavachari, K.; Foresman, J. B.; Cioslowski, J.; Ortiz, J. V.; Stefanov, B. B.; Liu, G.; Liashenko, A.; Piskorz, P.; Komaromi, I.; Gomperts, R.; Martin, R. L.; Fox, D. J.; Keith, T.; Al-Laham, M. A.; Peng, C. Y.; Nanayakkara, A.; Gonzalez, C.; Challacombe, M.; Gill, P. M. W.; Johnson, B. G.; Chen, W.; Wong, M. W.; Andres, J. L.; Head-Gordon, M.; Replogle, E. S.; Pople, J. A. *Gaussian 98*; Gaussian, Inc.: Pittsburgh, PA, 1998.
(15) Dove, M. F. A.; Creighton, J. A.; Woodward, L. A. *Spectrochim. Acta* **1962**, *18*, 267.
(16) Barnes, A. J.; Hallam, H. E. *Trans. Faraday Soc*. **1970**, *66*, 1920.
(17) Filgueira, R. R.; Fournier, L. L.; Varetti, E. L. *Spectrochim. Acta* **1982**, *38A*, 965.
(18) Maillard, D.; Schriver, A.; Perchard, J. P.; Girardet, C. *J. Chem. Phys*. **1979**, *71*, 505.
(19) Ault, B. S. *Rev. Chem. Intermed.* **1988,** *9*, 233.
(20) Pimentel, G. C.; McClellan, A. L. *The Hydrogen Bond*; W. H. Freeman: San Francisco, CA, 1960.
(21) Barnes, A. J.; Hallam, H. E.; Howells, J. D. R.; Scrimshaw, G. F. *J. Chem. Soc., Faraday Trans. 2* **1973**, *69*, 738.
(22) Barnes, A. J. *J. Mol. Struct*. **1983**, *100*, 258.
(23) Ault, B. S.; Pimentel, G. C. *J. Phys. Chem.* **1973**, *77*, 57.
(24) Ault, B. S.; Everhart, J. B. *J. Phys. Chem*. **1996**, *100*, 15726.